Electronic Supplementary Material (ESI) for Nanoscale.

Supplementary Information

A novel cell-scale bio-nanogenerator based on electron-ion interaction for fast light power conversion

Yu-Tao Li[a], He Tian[a], Hai-Ming Zhao[a], Mu-Qiang Jian[b], Yu-Jia Lv[c], Ye Tian[a], Qian Wang[a], Yi Yang[a], Yan Xiang[c], Yingying Zhang[b]*, Tian-Ling Ren[a]**

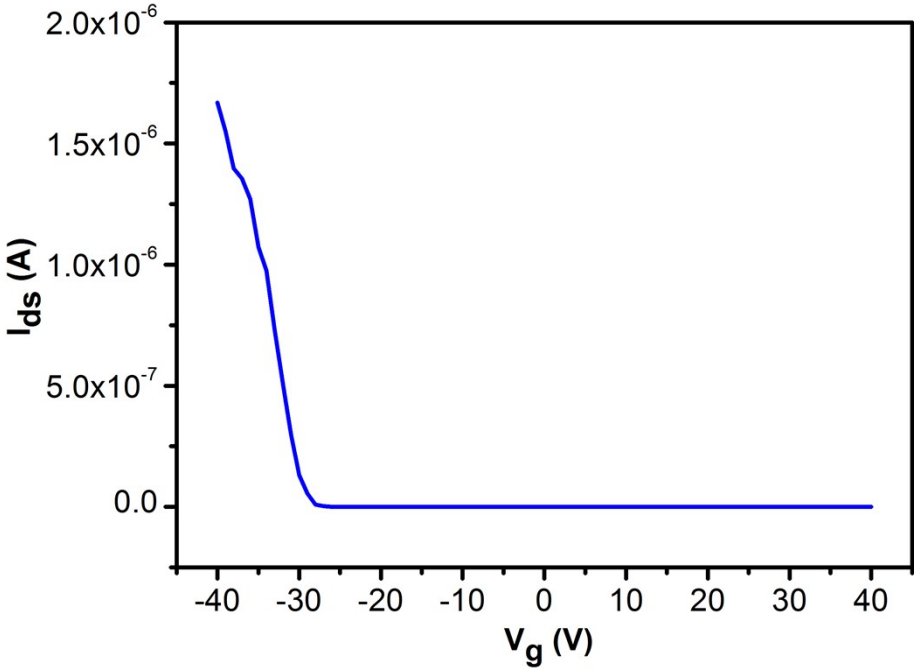

Figure S1. The transfer curve of as-grown CNTs MOSFET. The mobility of CNTs calculated from the formula $\mu = \frac{L^2}{CV_{ds}} \cdot \frac{\partial I_{ds}}{\partial V_{gs}}$ can reach as high as 586 $cm^2\ V^{-1}\ s^{-1}$, in which $C \approx \frac{2\pi\varepsilon\varepsilon_0 L}{\ln(2h/r)}$, L= 80 μm, r = 1.31nm, h = 300, ε ≈ 2.5, V_{ds} = 8V.

Table S1 Mobility of aligned or non-aligned CNTs

Materials	Mobility	Literatures
Non-aligned CNTs	~25 $cm^2\ V^{-1}\ s^{-1}$	ACS Appl. Mater. Interfaces 2016, 8, 27900−27910
Non-aligned CNTs	~30 $cm^2\ V^{-1}\ s^{-1}$	Nanoscale, 2017, 9, 4388–4396
Aligned CNTs	~510 $cm^2\ V^{-1}\ s^{-1}$	Nanoscale, 2016, 8, 13437–13444
Aligned CNTs	~586 $cm^2\ V^{-1}\ s^{-1}$	This work

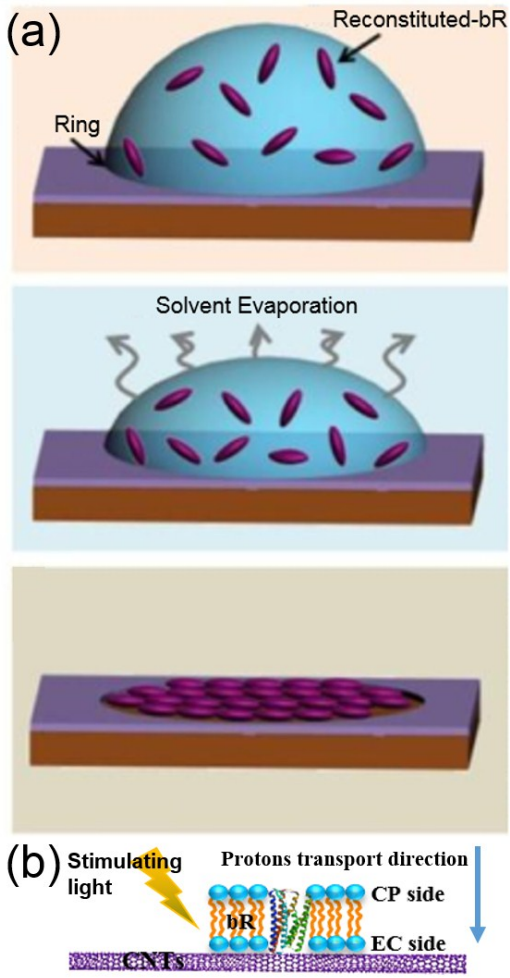

Figure S2. The schematics of (a) evaporation-induced assembly and (b) bR self-assemble orientation.

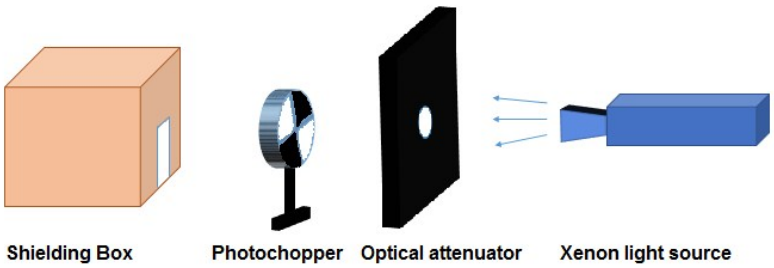

Figure S3. The schematic of measurement setup. The Xenon light source is from tungsten lamp (PLS-SXE250).The optical attenuator is used to adjust the light intensity and also results in a small light spot. The photochopper is used to control the light frequency which can change from 1Hz to 400 Hz. Finally, the shielding box of probe station is used to shield electromagnetic interference of surroundings.

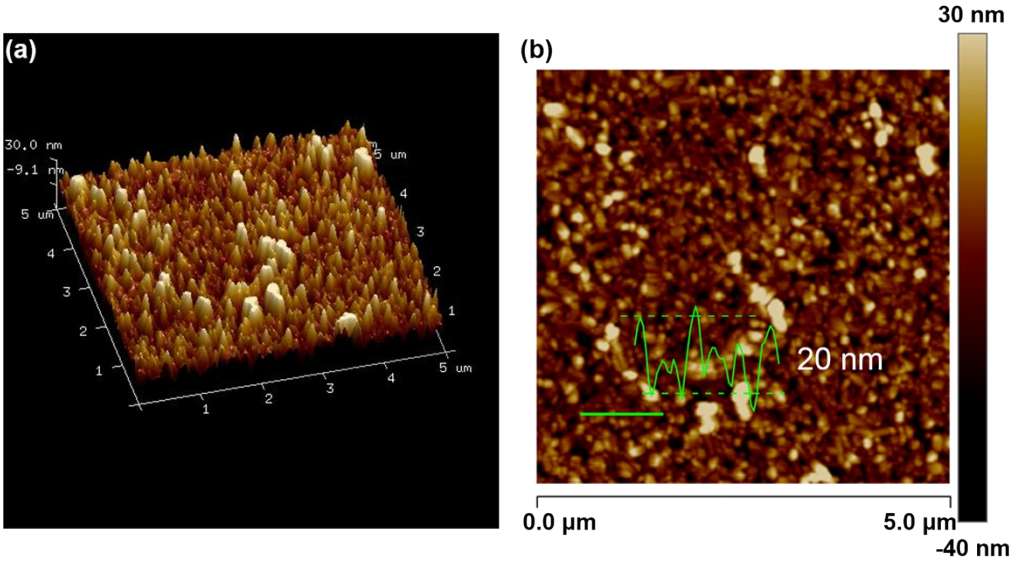

Figure S4. (a) The 3D AFM image and (b) 2D AFM image with height profile of the bR layer.

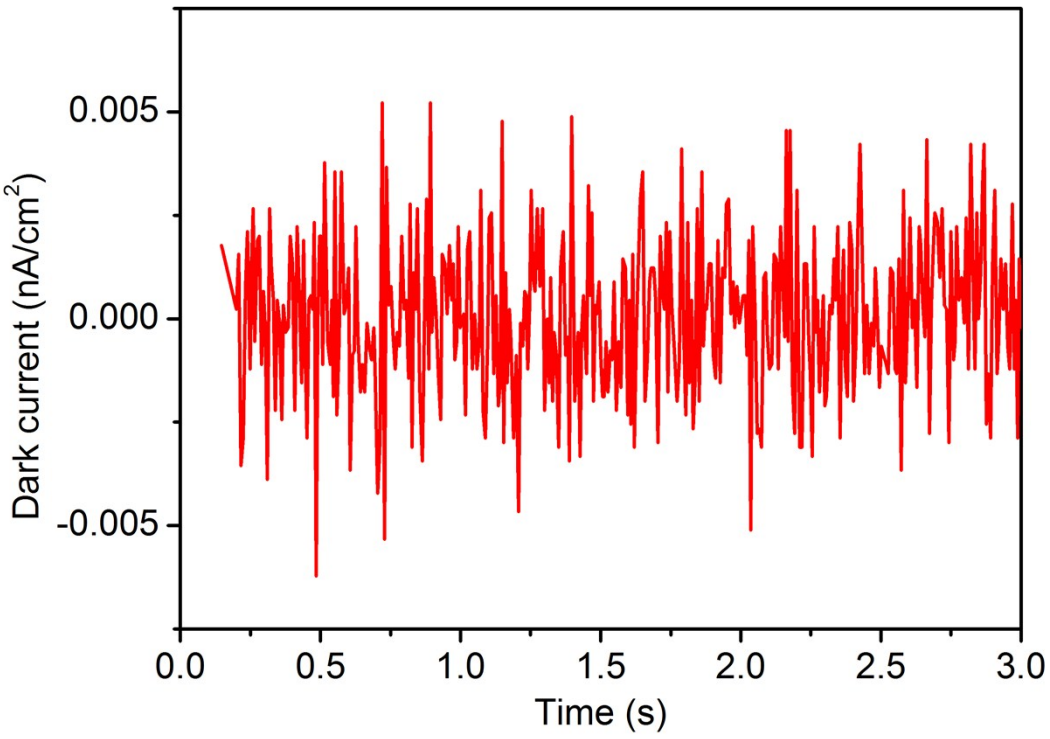

Figure S5. Dark current of the bR-CNTs biohybrid nanogenerator

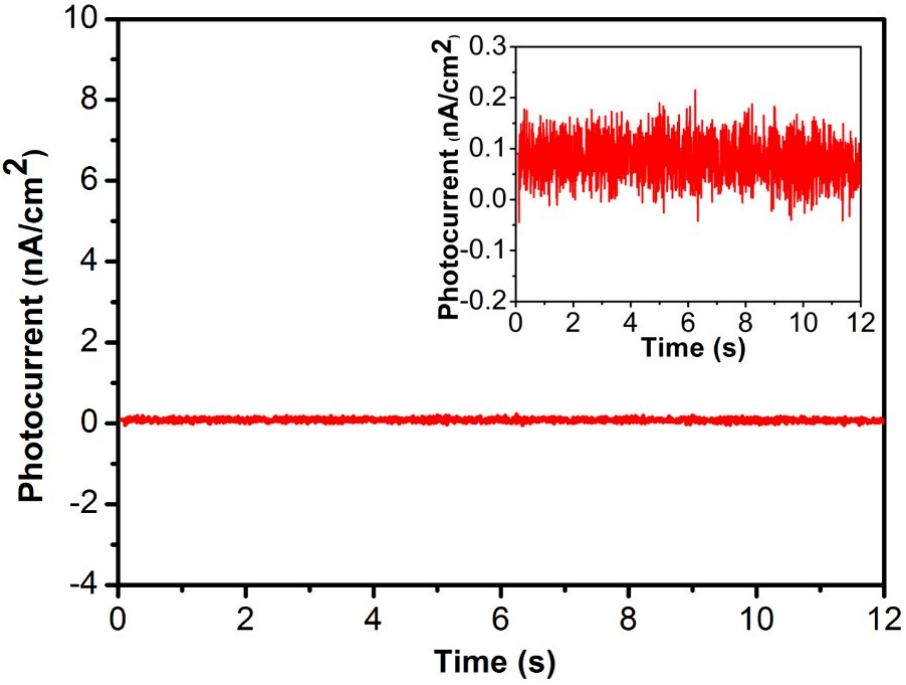

Figure S6. The photocurrent response of the device without bR layer. The insert figure shows the enlarged view of the data.

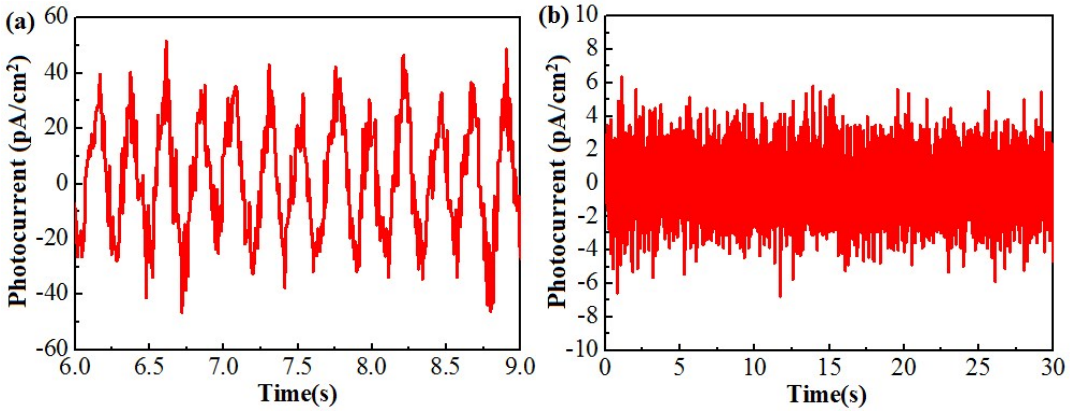

Figure S7. (a) The photocurrent tested from Cr/Au electrode when there is no Na_2SO_4 solution. (b) The photocurrent tested from bR side when there is no Na_2SO_4 solution. The low and unstable photocurrent response without Na_2SO_4 solution demonstrate the Na_2SO_4 solution is necessary to provide a biocompatible environment for the protein.

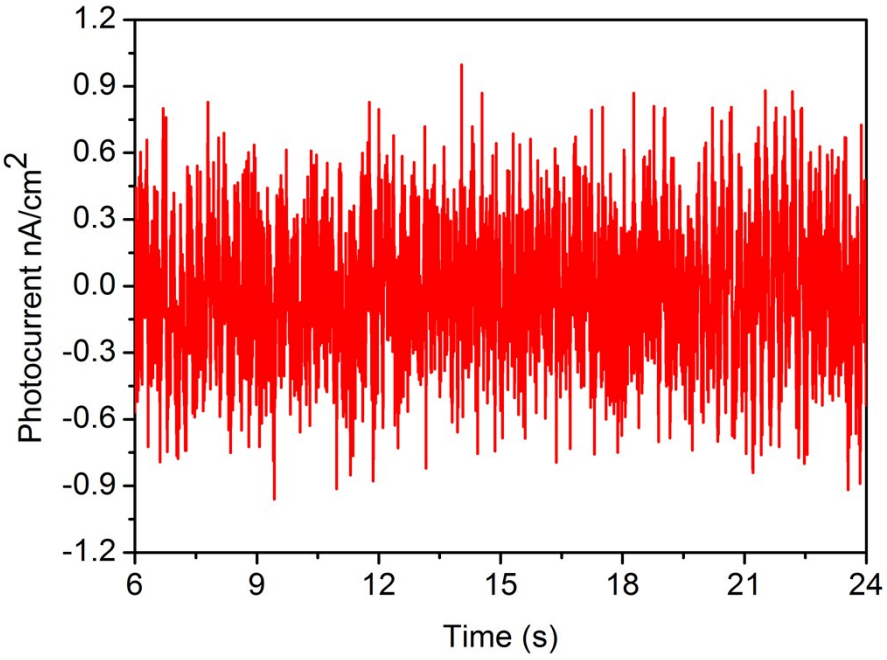

Figure S8. Photocurrents generated from bR biohybrid device based on ITO substrate under 2 Hz and 0.43 mW/cm^2 stimulating light.

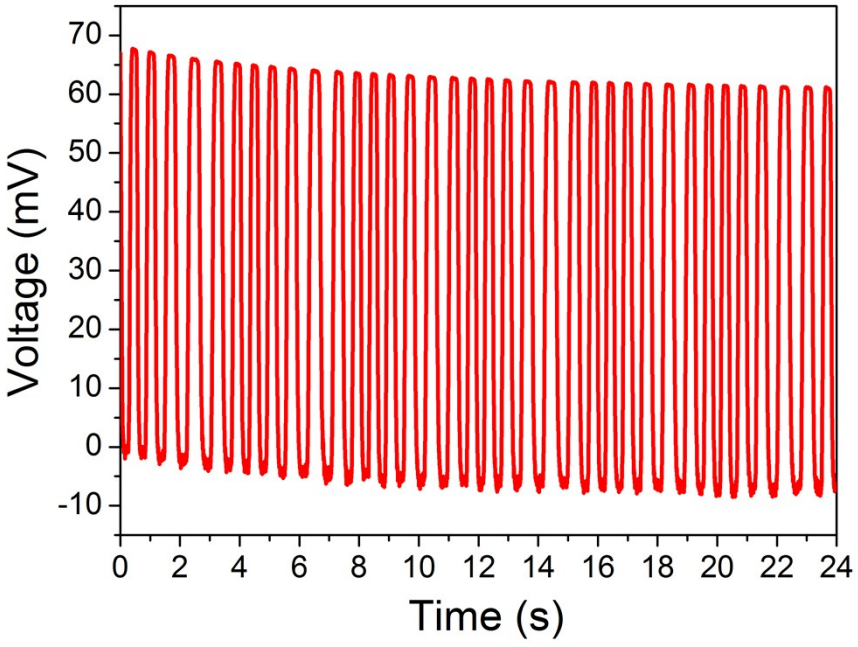

Figure S9. The voltage output of bR biohybrid nanogenerators.

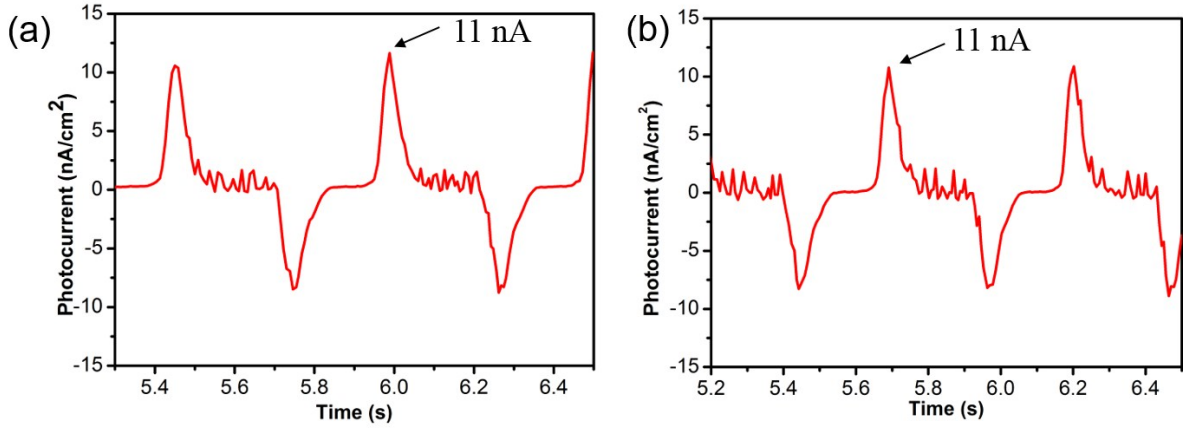

Figure S10. The photocurrent response of the (a) initial devices and (b) one month later

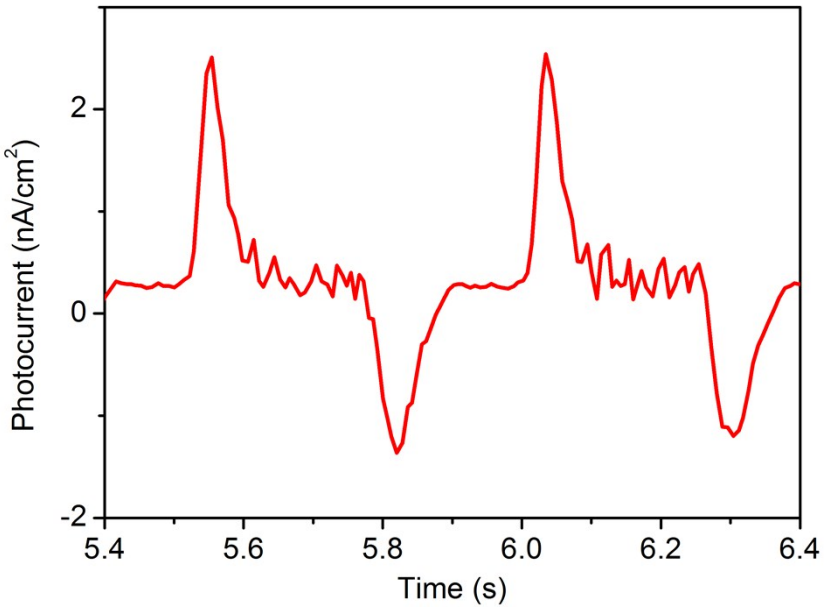

Figure S11. Photocurrent signal without Cr/Au electrode contact

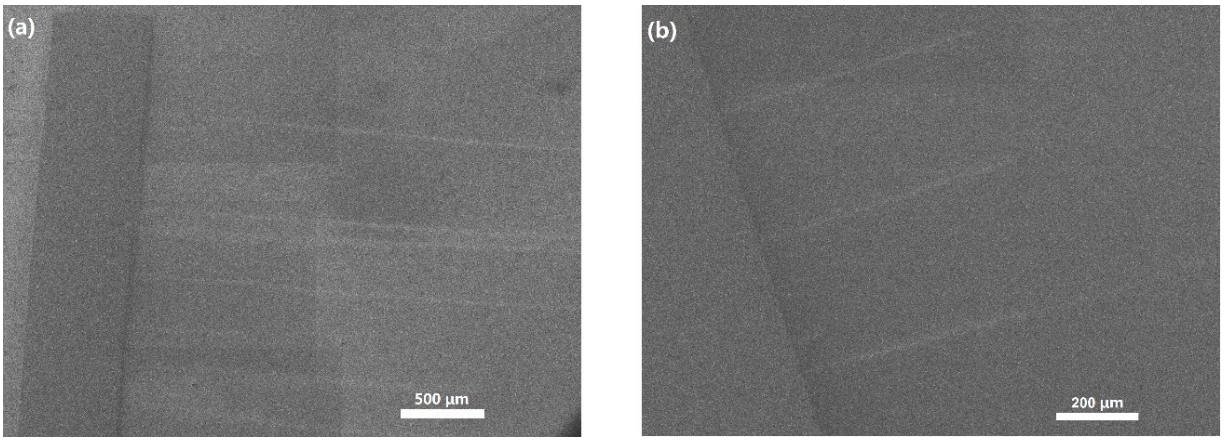

Figure S12. The morphology of electrode connecting with CNTs. (a) High density of CNTs (5 CNTs /mm). (b) Low density of CNTs (1 CNTs /mm).

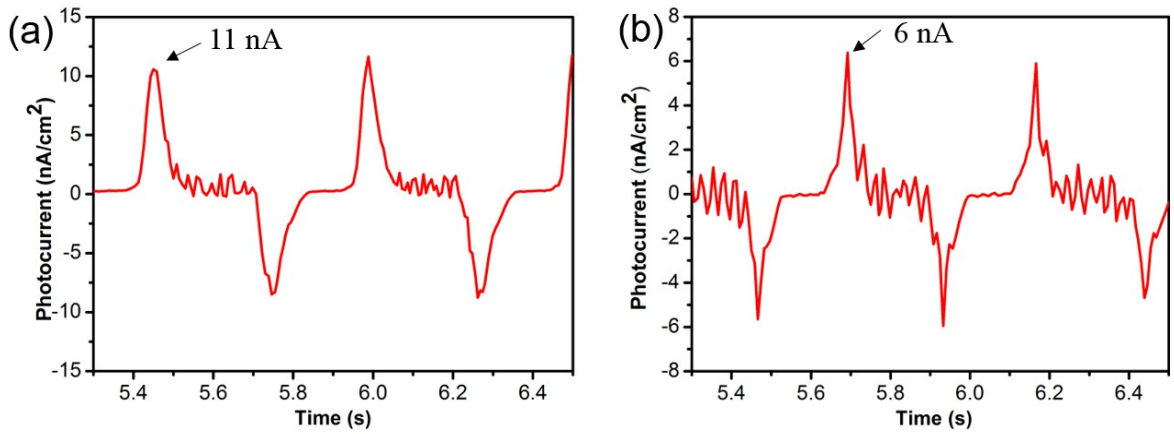

Figure S13. In order to test the device-to-device variability, besides the two devices described in our manuscript, we fabricated another device (Sample C) to verify the repeatability of our devices. The photocurrent responses of (a) Sample A and (b) Sample C are shown in the Figure above. The measurements were performed both under 2 Hz, 0.43 mW/cm^2 flicking light condition. The photocurrent peak intensity of two high performance devices are at the same level (around 10 nA/cm^2). The peak photocurrent value of these devices are influenced by the CNTs density and length, which demonstrates that stable devices performance can achieve by controllable CNTs growing process.

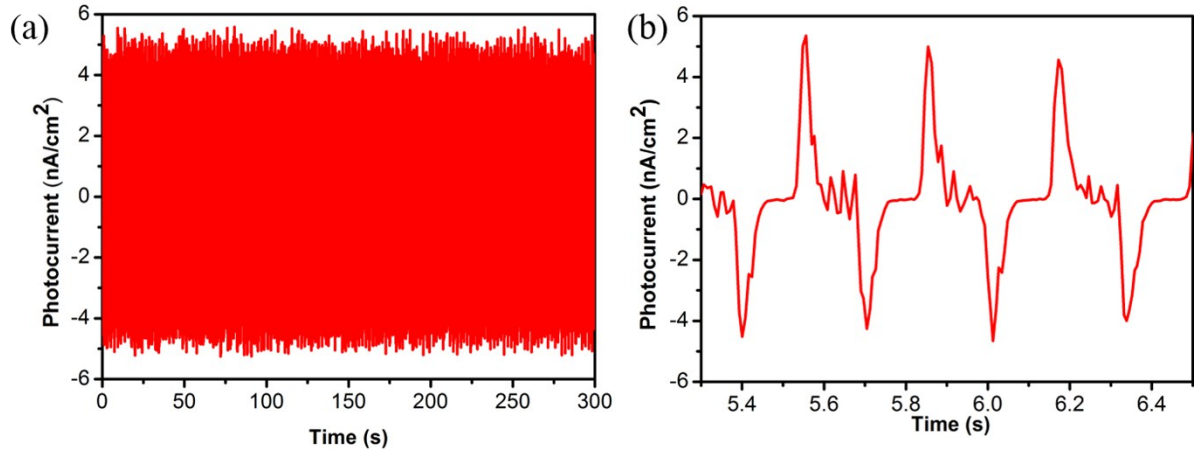

Figure S14. The photocurrent response of the device (a) under longer timeframes and (b) the enlarged view of it. The measurements were performed both under 4 Hz, 0.43 mW/cm^2 flicking light condition. It can be claimed that the device shows stable performance at long times after a lot of illumination.

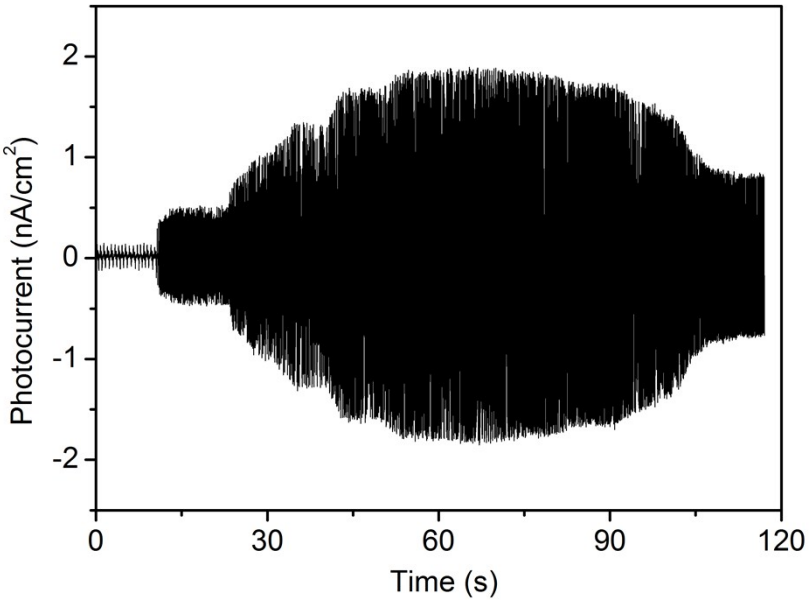

Figure S15. The relationship between photocurrent of low density CNTs device and the frequency of stimulating light. The variation regulation matches the photocurrent of high density CNTs well.

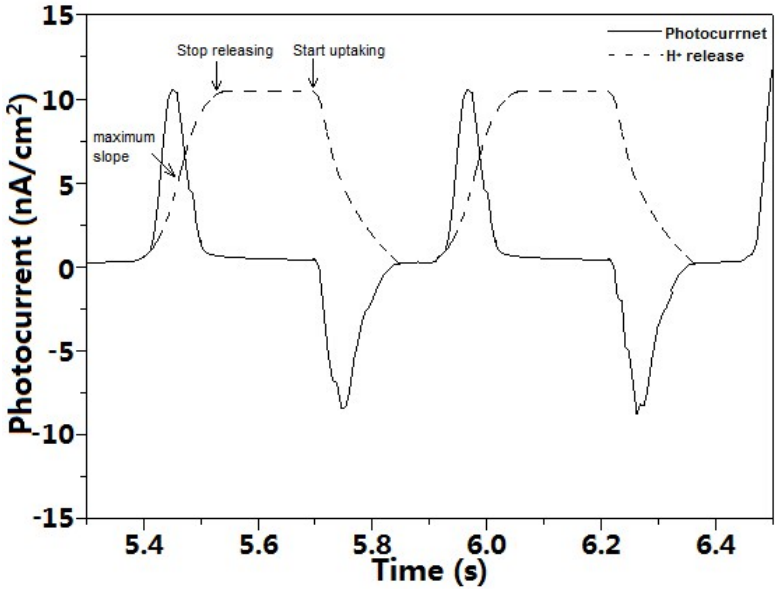

Figure S16. The whole H^+ ions generation transport process. The solid line stands for the photocurrent and the dashed line stands for the H^+ releasing process. The slope of H^+ ions releasing increases initially and then decreases. The maximum slope of H^+ releasing corresponds to the peak of photocurrent.

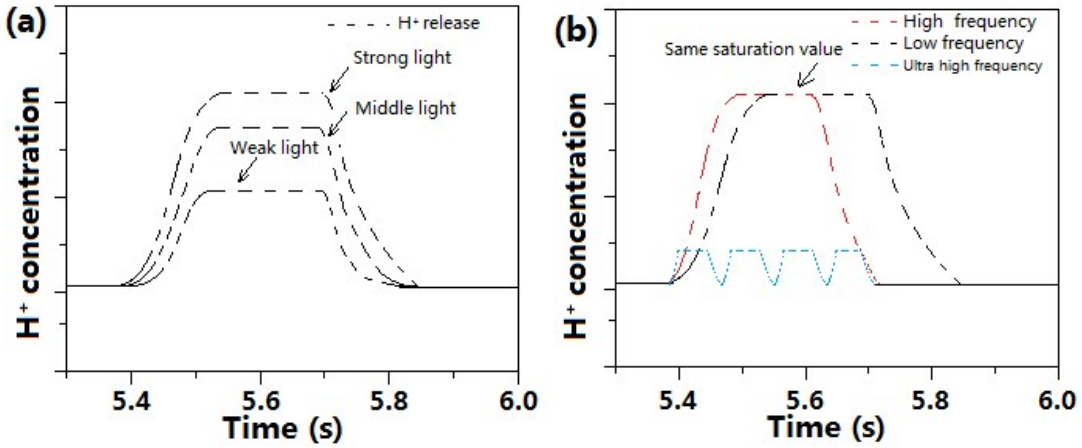

Figure S17. H^+ ions transport process under different light (a) intensity and (b) frequency. The maximum H^+ releasing slope increases with light intensity as well as lower frequency and H^+ releasing cannot reach the maximum slope at higher frequency (> 50 Hz).